Robust control for the air path of a downsized engine

Guillaume Colin, Yann Chamaillard, Benoit Bellicaud

Robust control for the air path of a downsized engine

Guillaume Colin*, Yann Chamaillard, Benoit Bellicaud

Institut Pluridisciplinaire de Recherche en Ingénierie des Systèmes, Mécanique, Energétique (PRISME), EA4229 University of Orléans, 8, rue Léonard de Vinci, 45072 Orléans, France

Abstract

This paper presents a simple method for designing a robust controller that can be used on nonlinear systems, here the air path of a downsized engine. This computationally inexpensive controller is thus obtained faster and more systematically than the usual look-up-table based controllers. The successive steps of the method are: system identification, system normalization and linearization, nominal model design, model uncertainty design, and controller design with property verification. This robust controller is applied to the air path of a downsized spark ignition engine, i.e. intake manifold pressure control and boost pressure control.

Key words: Engine Control, Robust Control, PID, Uncertainty model, Nonlinear systems.

*Corresponding author.

Email addresses: guillaume.colin@univ-orleans.fr (Guillaume Colin), yann.chamaillard@univ-orleans.fr (Yann Chamaillard), benoit.bellicaud@univ-orleans.fr (Benoit Bellicaud)

1. Introduction

More stringent standards are being imposed to reduce the fuel consumption and pollutant emissions of spark ignition (SI) engines. Modern automobile engines must therefore meet the challenging, and often conflicting, goals of minimizing pollutant emissions and fuel consumption while satisfying driving performance over a wide range of operating conditions. Engine downsizing is one of the most effective strategies for improving fuel economy while maintaining the advantage of the low emission capability of three-way catalytic systems and combining several well known technologies [1]. Downsizing is the use of a smaller capacity engine operating at higher specific engine loads, i.e. at better efficiency points [2]. Turbocharging is one of the relevant ways to achieve efficient downsizing [3]. Moreover, engine control is necessary to achieve an efficient engine torque control [4], which includes in particular the control of ignition coils, fuel injectors and air actuators (throttle, turbocharger, etc).

1.1. System description

The air intake of a turbocharged SI engine, represented in Figure 1 can be described as follows. The compressor (pressure p_{boost}) produces a flow from the ambient air (pressure p_{amb}). The compressor flow is cooled down by an intercooler and goes through the throttle Th into the intake manifold (pressure p_{man}). At the exhaust side, the exhaust flow is split in two parts: the turbine flow and the wastegate flow. The turbine flow powers up the turbine and through a shaft drives the compressor. Thus, the supercharging pressure p_{boost} can be adjusted by the turbine flow which is controlled by the

wastegate WG.

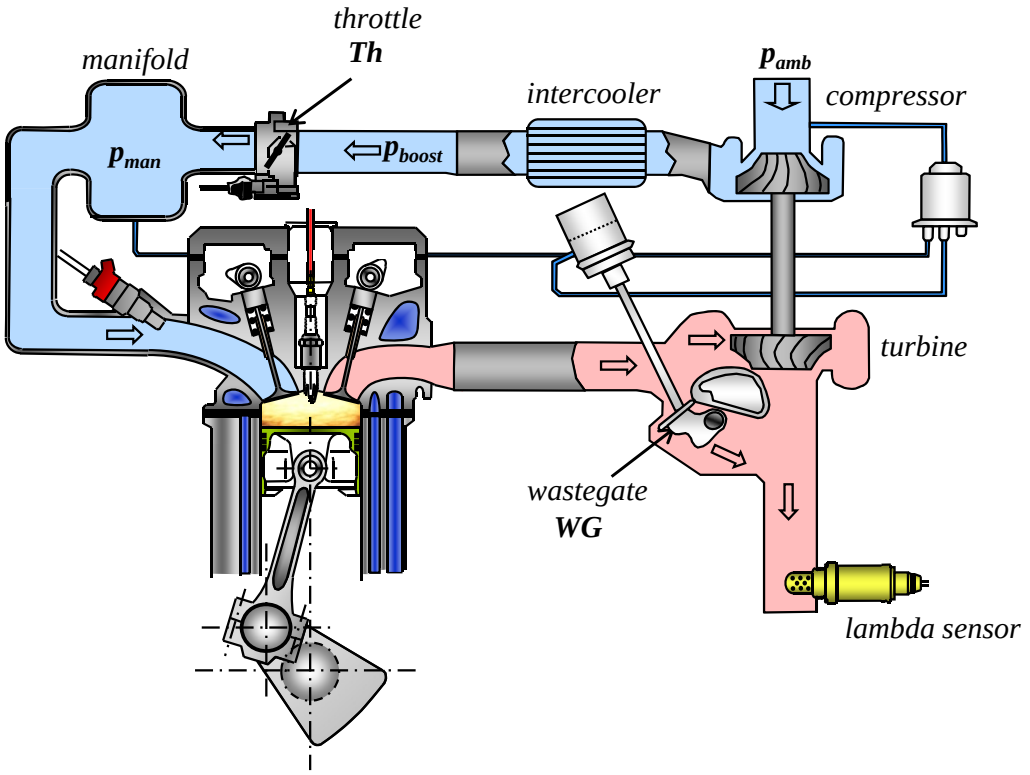

Figure 1: Air intake of a turbocharged SI engine

All of the results presented here were produced with a 0.6 Liter turbocharged 3 cylinder MCC Smart engine. A complete torque control is necessary to test the proposed method (control of ignition coils, injectors, throttle position). This was implemented on the engine test bench through a fast prototyping system based on xPCTarget from Matlab®. It is worth noting that the Air Fuel Ratio (AFR) control must be very accurate to limit overshoot and undershoot of the AFR. The throttle actuator control will not presented here. In this engine configuration, the wastegate valve, which is

linked to a membrane, is pneumatically controlled with a three way electro-valve connected between boost pressure and atmospheric pressure as shown in figure 1.

1.2. Problem formulation

As cylinder pressure sensor is not available, the intake manifold pressure p_{man} becomes the most measurable image of the engine torque. Hence, the air path control manipulates the intake manifold pressure. For a given intake manifold pressure p_{man}, there is an infinite number of solutions for opening the actuators, but only one is optimal from the energy point of view. To reach maximum efficiency, the throttle Th should be wide open. Engine control should therefore maintain the throttle open when $p_{boost} > p_{amb}$ in order to reduce pumping losses in steady state. It is worth noting that the throttle is open when $p_{boost} \approx p_{man}$. This implies that the supercharging pressure target is the same as the intake manifold pressure target. This is a pure fuel consumption minimization choice without regarding the transient performance. Another solution will be to adapt the boost pressure set point function of the desired efficiency loss as in [5]. In this case an efficiency loss of 0% corresponds to a pure fuel consumption choice.

Therefore, the control is multiobjective: to have the maximum opening of the throttle and to track the intake manifold pressure target. Moreover, this nonlinear system considered has subsystems with very different dynamics: the response time of the subsystem intake/throttle is much smaller than that of the subsystem turbocharger/wastegate.

The actuators to be controlled are the throttle and the wastegate, that have saturations which must be taken into account for the controller design. The

global control scheme for the air path of a turbocharged SI engine is shown on figure 2. The torque set point is directly linked to the driver's request. Then, the supervisor provides an air mass set point which is next translated into an intake manifold pressure set point p_{man_sp}. For the intake manifold pressure controller, the manipulated variable is the throttle position set point Th and the controlled variable is the intake manifold pressure p_{man}. For the boost pressure controller, the manipulated variable is the wastegate set point WG and the controlled variable is the supercharging pressure p_{boost}.

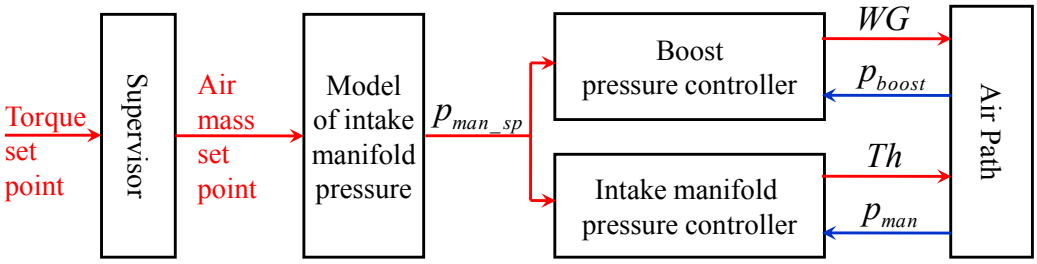

Figure 2: Global scheme for the air path control of the turbocharged SI engine

1.3. Main contributions

To control the air path of a spark ignition engine, various solutions have been proposed in the literature. For turbocharger control, in [6], a state feedback control is proposed using a physical model of the turbocharger. However, in this control scheme, which has been tested only in simulation, the fastest response is not produced with a wide open throttle and a fully closed wastegate [7]. In addition, at a steady speed, the throttle is not wide open; as discussed above, however, this is an important point in reducing fuel consumption. In [8], a variable feedforward plus a PI controller (based on

exhaust pressure) is proposed for an engine with a Variable Geometry Turbine (VGT). In spite of tuning difficulties / problems, this control scheme, which has only been tested in simulation, gives quite good results. In [9], an Internal Model Control is used for the intake manifold pressure and Neural Linearized Predictive Control is used for the boost pressure. This control scheme, tested on an engine test bench and compared to the proposed controller, gives excellent performance results, but can pose some problems for the calibration of series vehicles. In [10], a control based on physical model is used for the boost pressure control and was tested on a vehicle. This scheme can also pose some calibration problems on series vehicles. Finally, as simple PID controllers [11] generate overshoots as shown in [12], gain-scheduling PID controllers, widely used in industry, could be used. Nevertheless, they are not easy to tune and are problematic for calibration and robustness.
In the literature, robustness, fast tuning and low computational cost are not always ensured all together. That is why, in this paper, we propose a method to synthesize a computationally inexpensive robust controller obtained faster and more systematically than the usual look-up-table based controllers, for a downsized Spark Ignition engine. This simple method, which ensures that the control is robust, can have a wide domain of application. In the proposed control scheme, based on linear control theory [13], the system nonlinearities will be represented by an average linear model with uncertainties.

The different steps for the controller design are detailed in the following :

- normalization and linearization (section 2),
- nominal model design (section 3),

- uncertainty representation (section 4),
- controller design (section 5).

Section 2 assumes linearization and normalization of the system, which will have a consequence for system identification and nominal model design. Hence, the nonlinear system will be excited on all operating points in order to identify the normalized systems (section 3). From these data, a nominal linear model is computed and next the uncertainties are modeled (section 4). Consequently, the controller can be synthesize with stability proof (section 5). In the last part of the paper, control results are shown first in simulation and next on an engine test bench.

2. Normalization and linearization

The normalization and linearization step, based on [13], considers a single input single output (SISO) system governed by an ordinary differential equation (ODE):

$$\begin{cases} \frac{dz(t)}{dt} = f\left(z(t), v(t)\right) \\ w(t) = g\left(z(t), v(t)\right) \end{cases} \tag{1}$$

where $z(t)$ are the states, $v(t)$ is the input and $w(t)$ the output. This model can be normalized around an operating point z_0. A nominal constant input v_0 and a nominal constant output w_0 are associated to a nominal point z_0. The following normalized system can be then considered:

$$\begin{cases} \frac{dx(t)}{dt} = f_0\left(x(t), u(t)\right) \\ y(t) = g_0\left(x(t), u(t)\right) \end{cases} \tag{2}$$

Three new variables $x(t)$, $y(t)$ and $z(t)$ are so introduced:

$$\begin{cases} z(t) = z_0 x(t) = z_0 \left(x_0 + \delta x(t)\right) \\ w(t) = w_0 y(t) = w_0 \left(y_0 + \delta y(t)\right) \\ v(t) = v_0 u(t) = v_0 \left(u_0 + \delta u(t)\right) \end{cases} \tag{3}$$

where $x(t)$ are the states, $u(t)$ is the input and $y(t)$ the output. The hypothesis of only small deviations from the normalized equilibrium points is made. In equation (3), x_0, y_0 and u_0 can be assumed equal to 1. An advantage of normalization is that it is possible to define easily a small difference, i.e. $\delta x(t) \ll 1$, $\delta y(t) \ll 1$ and $\delta u(t) \ll 1$ (notion of smallness).

Finally, the following linear model is defined:

$$\begin{cases} \frac{dx(t)}{dt} = Ax(t) + bu(t) \\ y(t) = cx(t) + du(t) \end{cases} \tag{4}$$

with $A \in \mathbb{R}^{n \times n}$, $b \in \mathbb{R}^{n \times 1}$,$c \in \mathbb{R}^{1 \times n}$,$d \in \mathbb{R}$, where:

$$\begin{cases} A = \frac{\partial f_0}{\partial x}\Big|_{x=x_0,u=u_0} & b = \frac{\partial f_0}{\partial u}\Big|_{x=x_0,u=u_0} \\ c = \frac{\partial g_0}{\partial x}\Big|_{x=x_0,u=u_0} & d = \frac{\partial g_0}{\partial u}\Big|_{x=x_0,u=u_0} \end{cases} \tag{5}$$

Describing a real dynamic system using a normalized and linearized mathematical model is convenient for the analysis and synthesis of appropriate control systems. However, the controller obtained with this normalized and linearized system cannot be directly applied to the real system. Therefore, normalization and de-normalization blocks have to be added on a classical closed loop control scheme. The interface is shown in figure 3.

Firstly, the normalization is chosen as (from (3)) :

$$\delta y(t) = \frac{w(t)}{w_0} - y_0 = \frac{w(t)}{w_0} - 1 \tag{6}$$

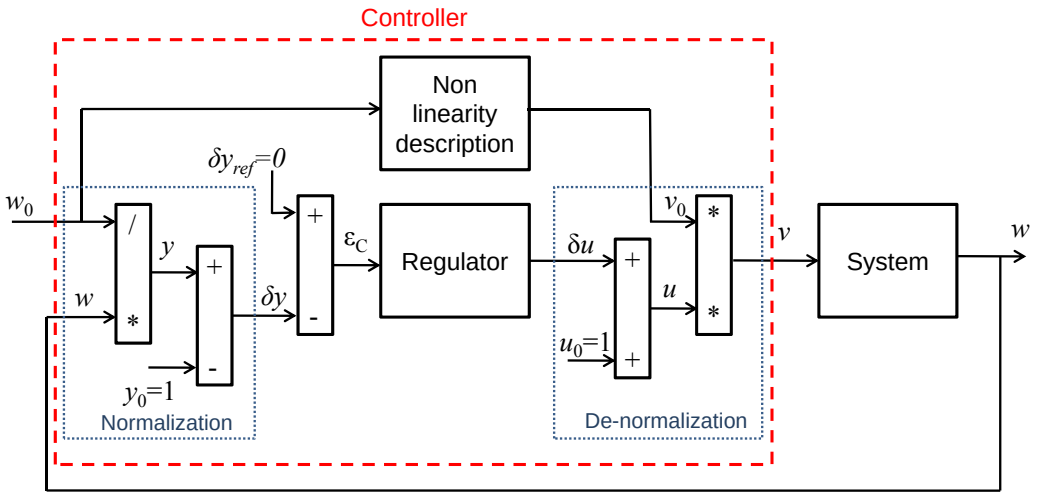

Figure 3: Interface between Linear normalized Controller with the nonlinear system

The error of the controller is therefore:

$$\epsilon_c(t) = \delta y_{ref} - \delta y(t) \tag{7}$$

where the reference δy_{ref} is equal to zero due to the normalization and linearization steps. Secondly, the de-normalization is chosen as (from (3)):

$$v = v_0(u_0 + \delta u) = v_0(1 + \delta u) \tag{8}$$

where δu is the output of the controller

Hence, the control scheme shown on figure 3 is equivalent to the one shown on figure 4. It can be seen that a gain scheduling controller appears in the proposed control scheme because the output of the regulator is multiplied by the nominal input v_0. This nominal input v_0 has been previously computed by a non linearity description (here a static look-up-table function of engine speed and intake manifold pressure set point). Moreover, a feedforward is

also present because the nominal input v_0 is added to the output of the controller u. As the normalization is done with respect to the set point, the reference must not be equal to zero, which is the case here for the air path of the turbocharged SI engine. A small variable change must be done for the nominal input v_0 to make it always different from zero (otherwise the controller will be inactive as shown in figure 4).

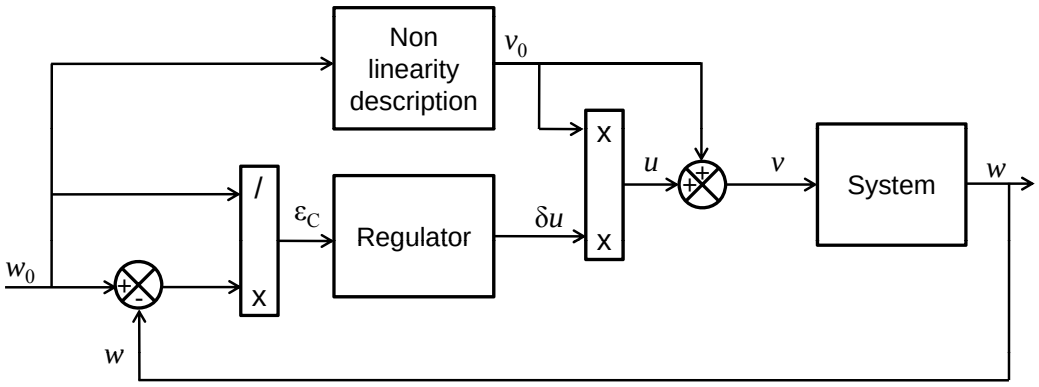

Figure 4: Equivalent proposed control scheme that points out a gain scheduling controller with a feedforward

3. Nominal model design

The step of linearization states that linear models are necessary to synthesize the control. Hence, all operating points will be swept to make the identification of these models. Here, a frequential identification is performed [14] on all the representative operating points: 52 for the throttle and 19 for the wastegate (some operating points are the same). The engine speed N_e goes from 1500 rpm to 4500 rpm and torque goes from 0 Nm to 90 Nm (minimum to maximum). Small engine speeds have been removed because

no boost pressure is available and because our engine brake is unstable in this domain. A multisinus excitation (sum of sinus at different frequencies) for the system input is performed while system output is acquired. Finally, Fast Fourier Transform (FFT) is used to obtain the frequential representation of the system (figures 5 and 6). Note that the average values of inputs and outputs are saved in order to compute the nonlinearity description of figure 4.

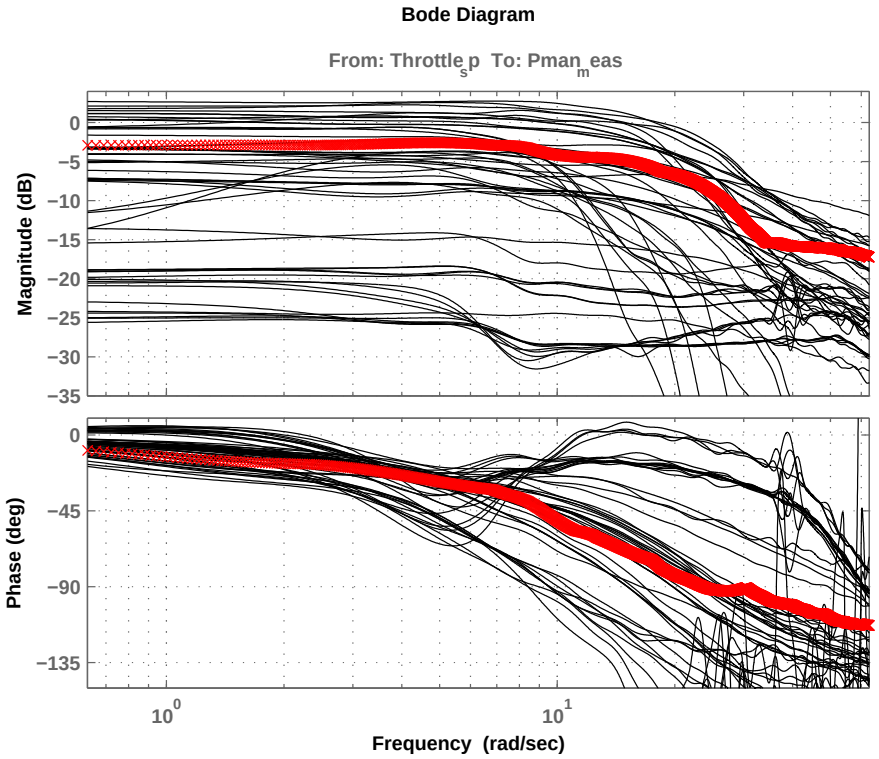

Figure 5: Bode diagram of the identified systems (black) and average system (red): system input is the normalized throttle set point and system output is the normalized intake manifold pressure

As frequency responses for all the representative operating points have

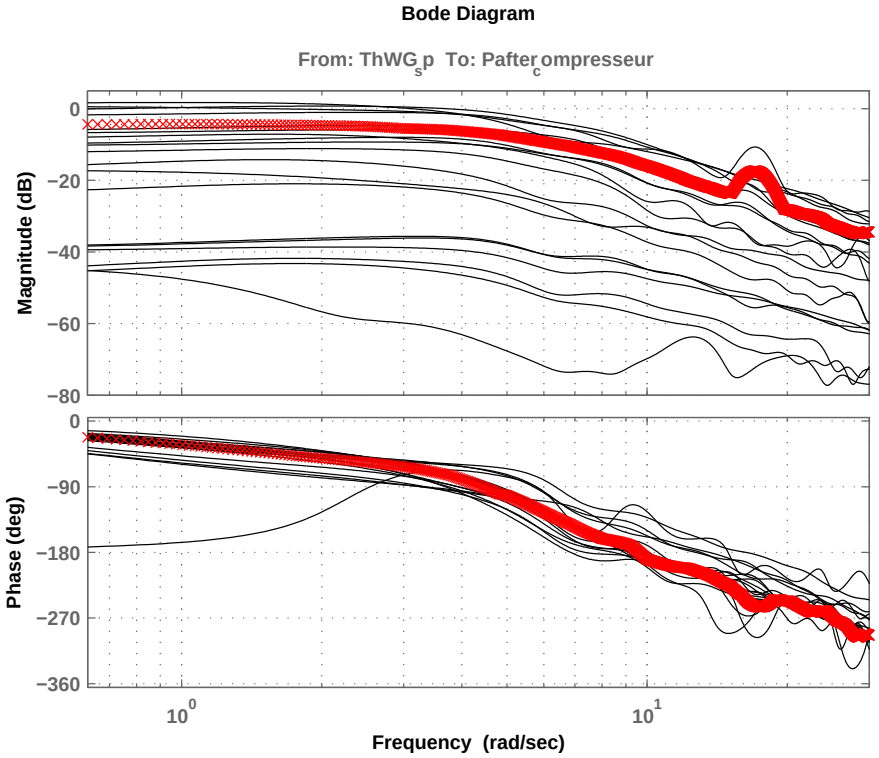

Figure 6: Bode diagram of the identified systems (black) and average system (red): system input is the normalized wastegate set point and system output is the normalized boost pressure

been acquired, the real frequential responses will be used to determine the nominal model and the uncertainty model. The reference system is chosen as the average between the maximum and the minimum system at each frequency (red system on figures 5 and 6). This choice (and not the average of all systems) is directly linked to the norm used to modelize uncertainties (13). This reference system, not physical, is a sequence of values, where each value corresponds to a behavior at one given frequency.

The reference system is then used to identify the average model, called

here nominal model. This model will be used for the controller design and will be defined as a continuous transfer function. The transfer function can be found using an optimization method with an appropriate criterion to minimize. The criterion to minimize is the weighted sum of root mean squared error (RMSE) of the magnitude and the RMSE of the phase, where the error is computed between the reference system and the nominal model. As the nominal model must be as simple as possible, a first or a second order transfer function can be chosen:

$$P_1(s) = \frac{b_0 + b_1 s}{1 + a_1 s} \tag{9}$$

$$P_2(s) = \frac{b_0 + b_1 s + b_2 s^2}{1 + a_1 s + a_2 s^2} \tag{10}$$

For the intake manifold pressure controller, a first order is sufficient, yielding the following transfer function (figure 7):

$$P_{Th}(s) = \frac{-0.005101 s + 0.8246}{0.09747 s + 1} \tag{11}$$

For the boost pressure controller, a second order is necessary, yielding the following transfer function (figure 7):

$$P_{WG}(s) = \frac{0.604}{0.05723 s^2 + 0.3115 s + 1} \tag{12}$$

Here, just by looking at the phases of the Bode diagrams (figure 7) one can see that the throttle Th to intake manifold pressure p_{man} system is a first order and the wastegate WG to boost pressure p_{boost} system is a second order.

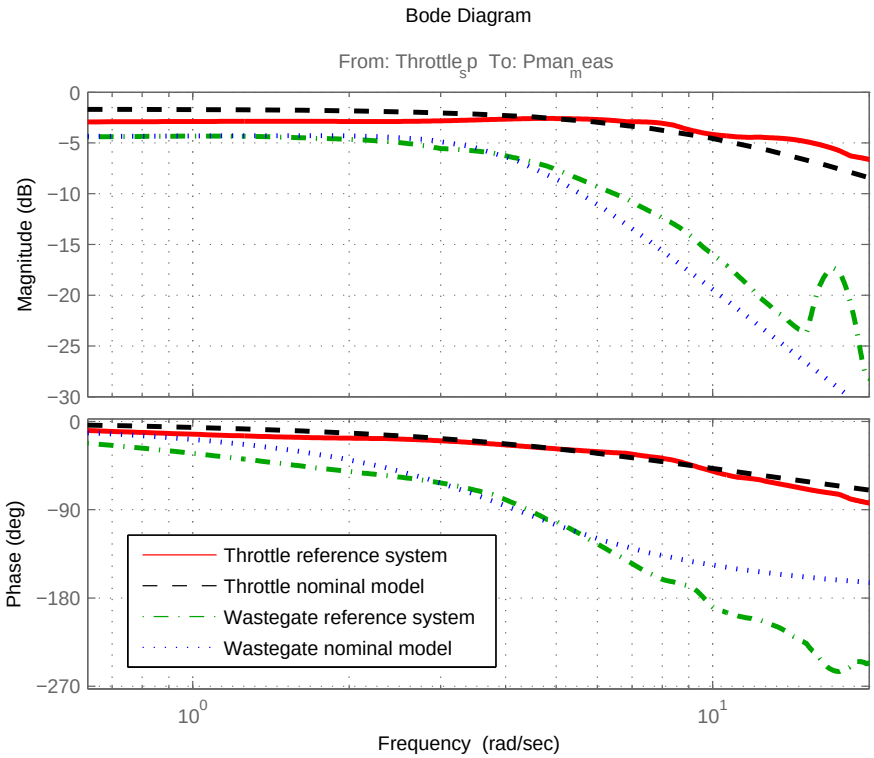

Figure 7: Identification results: bode diagram of the the reference system (from Th to p_{man} in red solid, from WG to p_{boost} in green dash dot) and of the identified linear model (from Th to p_{man} in black dash, from WG to p_{boost} in blue dot)

4. Uncertainty model design

A description of the uncertainties is necessary to allow the analysis of the closed loop system, especially the robustness property. In this work, the simplest method is used. The idea is to parameterize the uncertainty by the set:

$$S = \begin{cases} P(s)\,(1 + \Delta W(s)) \\ ||\Delta|| \leq 1 \\ arg\{\Delta\} \in [-\pi, \pi] \end{cases} \tag{13}$$

where $P(s)$ is the nominal model, $W(s)$ an uncertainty bound and Δ is the uncertainty generator. Here, the set is therefore defined by a nominal frequency response $P(s)$, a unit disc centered in the origin defined by Δ, and this disc is translated by $P(s)$ and scaled by a factor $P(s)W(s)$. Since for a fixed frequency the phase is not relevant due to the uncertainty circle around the nominal model, the magnitude may be used only to formulate a condition on the uncertainty bound $W(s)$. The uncertainty bound $W(s)$ is considered here as a first or a second order model computed from the measured maximum uncertainty as in [13] (Figures 8 and 9). Other uncertainties could be added in this model, e.g. aging of the system, variation of turbine or compressor characteristics, identification uncertainty.

The representation of the uncertainties around the nominal model is given in figure 10 for the throttle to intake manifold pressure system and in figure 11 for the wastegate to boost pressure system.

The uncertainty model for the intake manifold pressure controller is given by the following second order transfer function:

$$W_{Th}(s) = \frac{0.0005204s^2 + 0.1592s + 0.93671}{0.0007716s^2 + 0.1009s + 1} \tag{14}$$

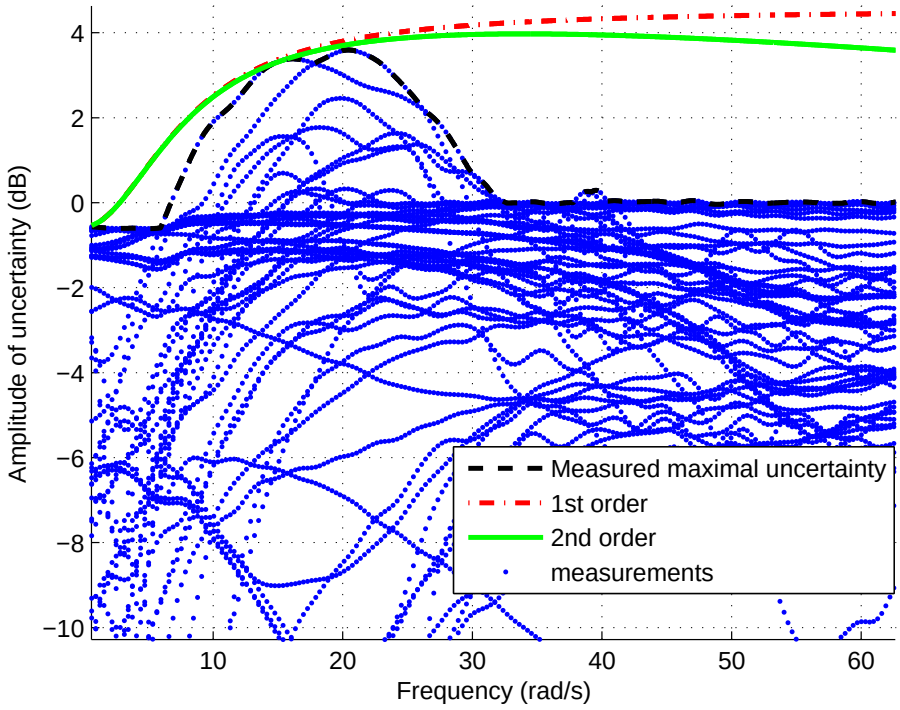

Figure 8: Amplitude of uncertainty (dB) versus frequency (rad/s) for the throttle to intake manifold pressure system

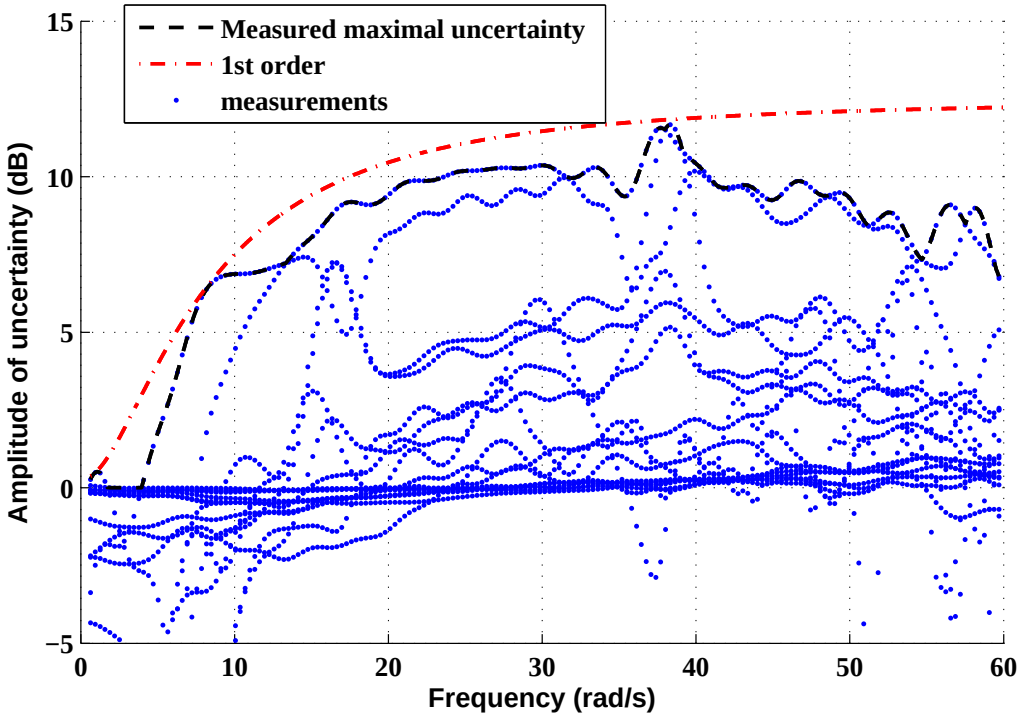

Figure 9: Amplitude of uncertainty (dB) versus frequency (rad/s) for the wastegate to boost pressure system

and the uncertainty model for the boost pressure controller by the following first order transfer function:

$$W_{WG}(s) = \frac{0.2578s + 1.031}{0.06098s + 1}. \tag{15}$$

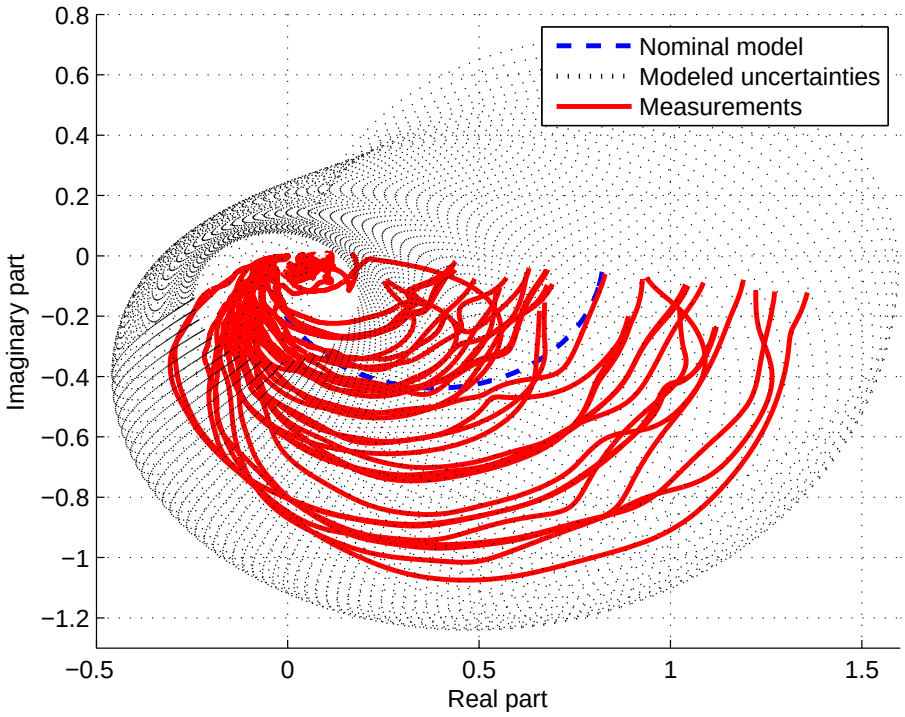

Figure 10: Nyquist diagram of the linear model with the modeled uncertainties for the throttle to intake manifold pressure system

5. Controller design

As seen before, the system has been normalized and linearized so that any linear controller, available in the linear control theory literature, could

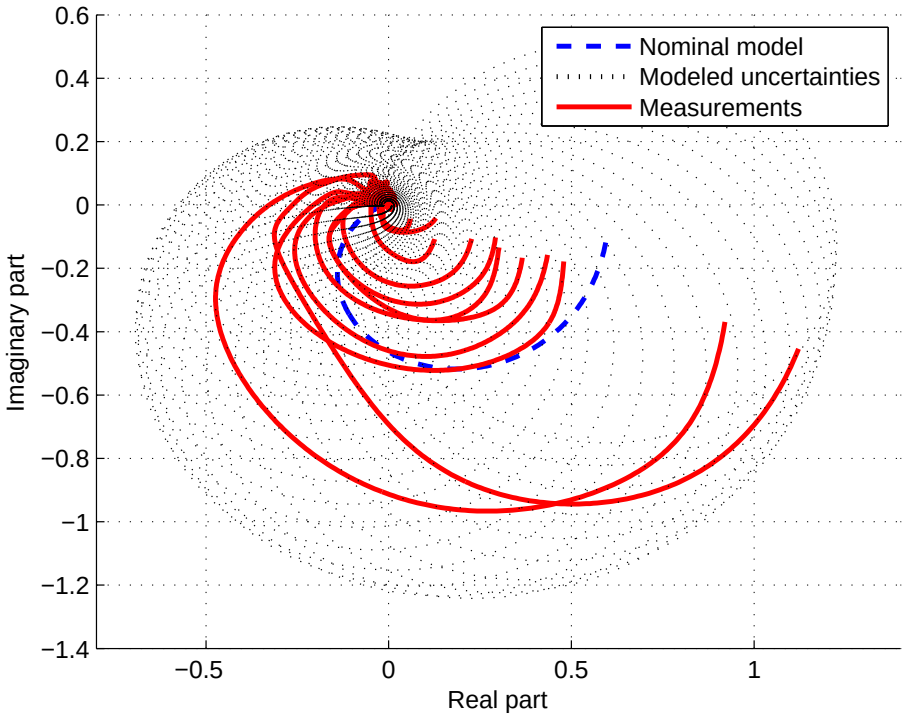

Figure 11: Nyquist diagram of the linear model with the modeled uncertainties for the wastegate to boost pressure system

be used in the control scheme of figure 4. The classical PID controller, tuned with a pole placement method in which robustness is verified, is chosen here for its simplicity and in order to prove the effectiveness of the proposed method. To avoid problems with the saturations, an anti-reset windup (ARW) has to be added to the controllers [15].

Assuming a nominal plant $P(s)$, a conservative bound on its uncertainty $W(s)$ and a controller $C(s)$ and assuming the nominal closed loop is asymptotically stable, the controller $C(s)$ will produce an asymptotically stable closed loop system for all the plants in the set S if the following inequality is verified for all frequencies (Nyquist stability theorem):

$$|1 + C(s)P(s)| \geq |C(s)P(s)W(s)| \tag{16}$$

Two cases of pole placement are here considered to find the coefficients K, T_i and T_d of the PID controller $C(s)$ (17), as shown in table 1.

$$C(s) = \frac{K(1 + sT_i + s^2T_iT_d)}{sT_i} \tag{17}$$

In this table, the computation of K, T_i and T_d is done while identifying $1 + C(s)F(s) = 0$ to the denominator of $G(s)$.

For the intake manifold pressure controller, as the nominal model is a first order, the desired (reasonable) system dynamic is chosen as a second order that ensures a robust control. For example, the parameters $\omega_n = 10rad/s$ and $\zeta = 1.2$ ensure robustness for the closed loop true system and for the closed loop nominal model with modeled uncertainties (i.e. (16) satisfied) as shown in figure 12. With this desired system the following coefficients of the PI controller are found $K = 1.4731, T_i = 0.1350$.

Open loop nominal system $F(s)$	$\frac{as+b}{cs+1}$	$\frac{a_3}{b_2s^2+b_1s+1}$
Desired closed loop system $G(s)$	$\frac{\omega_n^2}{s^2+2\zeta\omega_n s+\omega_n^2}$	$\frac{\alpha\omega_n^3}{(s^2+2\zeta\omega_n s+\omega_n^2)(s+\alpha\omega_n)}$
K	$\frac{2\zeta c\omega_n-1-a\omega_n^2 c/b}{b+a^2\omega_n^2/b-2\zeta a\omega_n}$	$\frac{\left(2\zeta\omega_n^2\alpha+\omega_n^2\right)b_1-1}{a_3}$
T_i	$\frac{Kb}{\omega_n^2(c+Ka)}$	$\frac{Ka_3}{\alpha\omega_n^3 b_1}$
T_d	0	$\frac{2\zeta\omega_n b_1+\alpha\omega_n b_1-b_2}{Ka_3}$

Table 1: Pole placement to find the coefficients of the PID controller

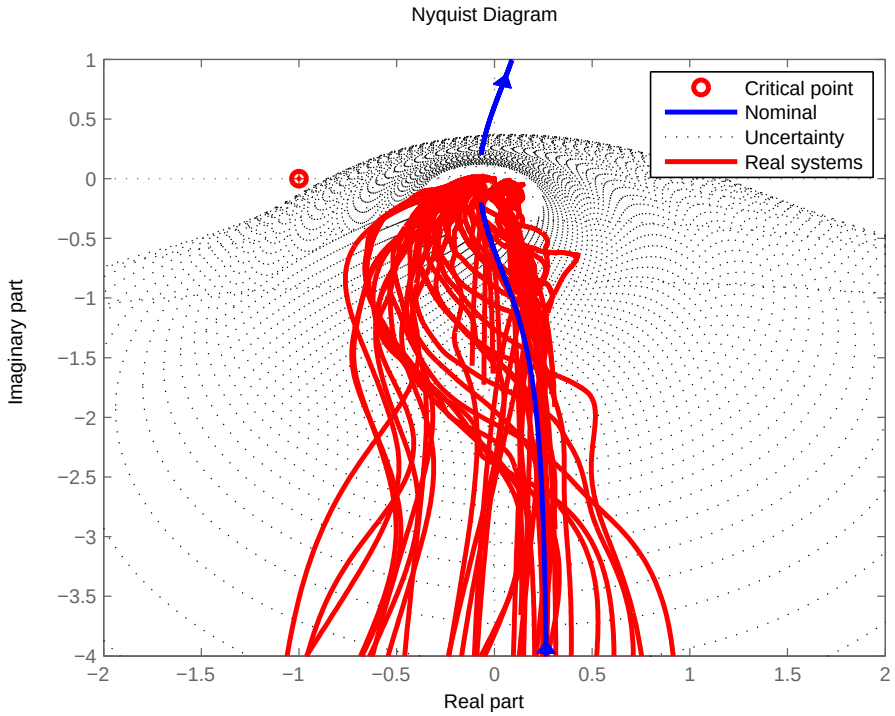

Figure 12: Nyquist representation of $C(s)P(s)$ for the intake manifold pressure controller: nominal model (blue), real systems (red), modeled system with circle amplitude of $|C(s)P(s)W(s)|$ around $C(s)P(s)$ (black)

For the boost pressure controller, as the nominal model is a second order, the desired (reasonable) system dynamic is chosen as a third order that ensures a robust control. For example, the parameters $\omega_n = 3rad/s$, $\zeta = 1.1$ and $\alpha = 1$ ensure robustness for the closed loop true system and for the closed loop nominal model with modeled uncertainties (i.e. (16) satisfied) as shown in figure 13. With this desired system the following coefficients of the PID controller are found $K = 1.0734, T_i = 0.4195, T_d = 0.3670$. The derivative of the controller has been filtered to avoid the classical high frequency problems. All the figures shown in this paper used the filtered derivate. A good margin of robustness is ensured for the closed loop system as shown in figure 13. Tuning parameter ω_n for boost pressure controller is smaller than for the intake manifold pressure controller, because desired dynamic are different.

Equation (16) is verified for each controller as shown on figure 14. In this figure, $|1 + C(s)P(s)|$ is always greater than $|C(s)P(s)W(s)|$ which proves the stability of the two closed loop systems.

6. Results

All of the results presented here were produced with a 0.6 Liter turbocharged 3 cylinder MCC Smart Engine (see section 1.1 for more details). In the presented results, both controllers runs together with the control scheme of figure 2.

Firstly, both controllers are validated in simulation on various transients. Figures 15 and 16 shows two examples of realized tests at two different engine speeds with variation of torque set point. The dynamic performance of both

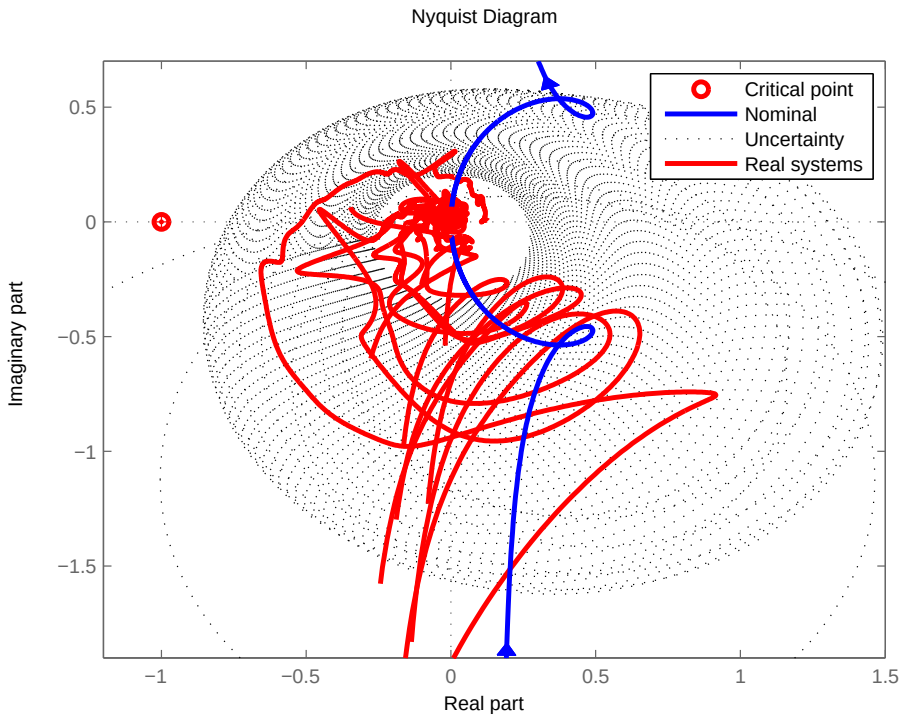

Figure 13: Nyquist representation of $C(s)P(s)$ for the boost pressure controller: nominal model (blue), real systems (red), modeled system with circle amplitude of $|C(s)P(s)W(s)|$ around $C(s)P(s)$ (black)

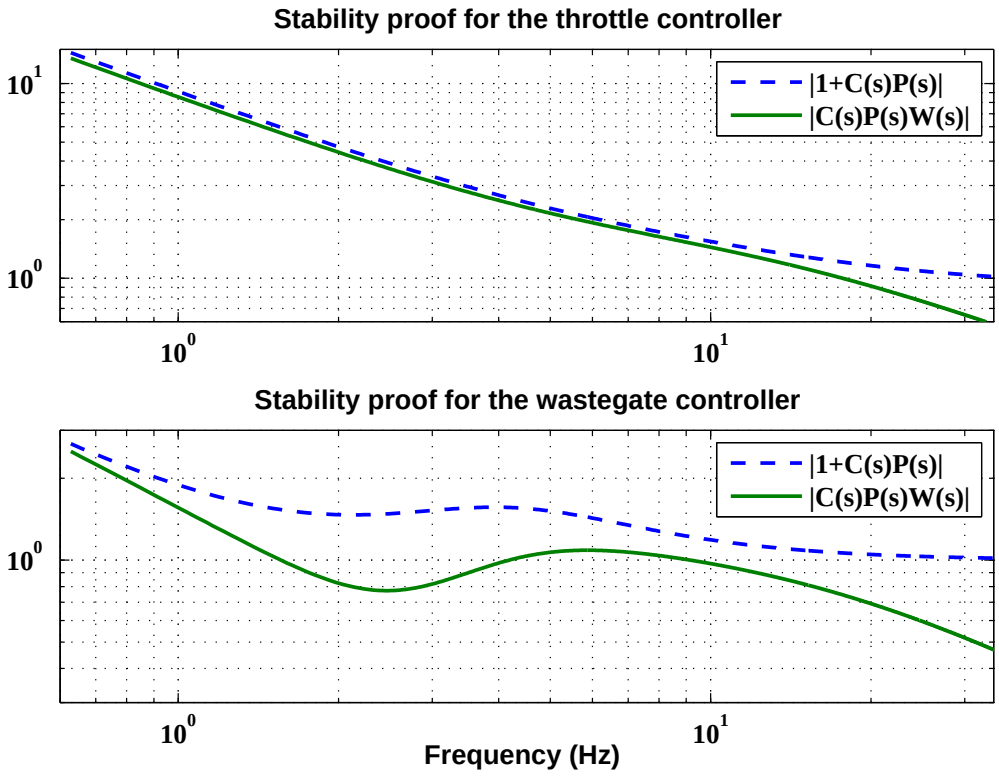

Figure 14: Nyquist stability proof (16) of designed controllers

controllers are quite good. Indeed, only a small overshoot of boost pressure appears (at 85s at the top of figure 16) and there is no steady state error.

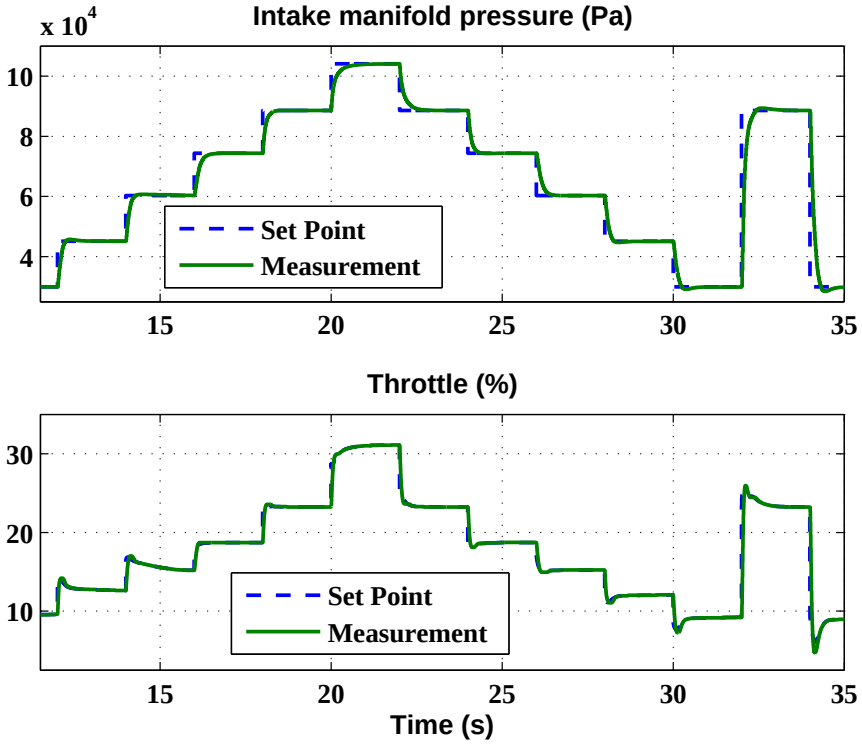

Figure 15: Simulation results at 3500rpm. Intake manifold pressure (Pa) vs. time (s) (top): set point p_{man_sp} (blue dash) and measurement p_{man} (green solid) ; Actuator position (%) vs. time (s) (bottom): throttle set point (blue dash), throttle position (green solid), wastegate fixed at 0% (not shown here)

Secondly, both controllers are validated on engine test bench on various transients. Two example of realized tests, where both controllers runs together, are shown here:

- variation of torque set point and engine speed (Figures 17, 18 and 19)

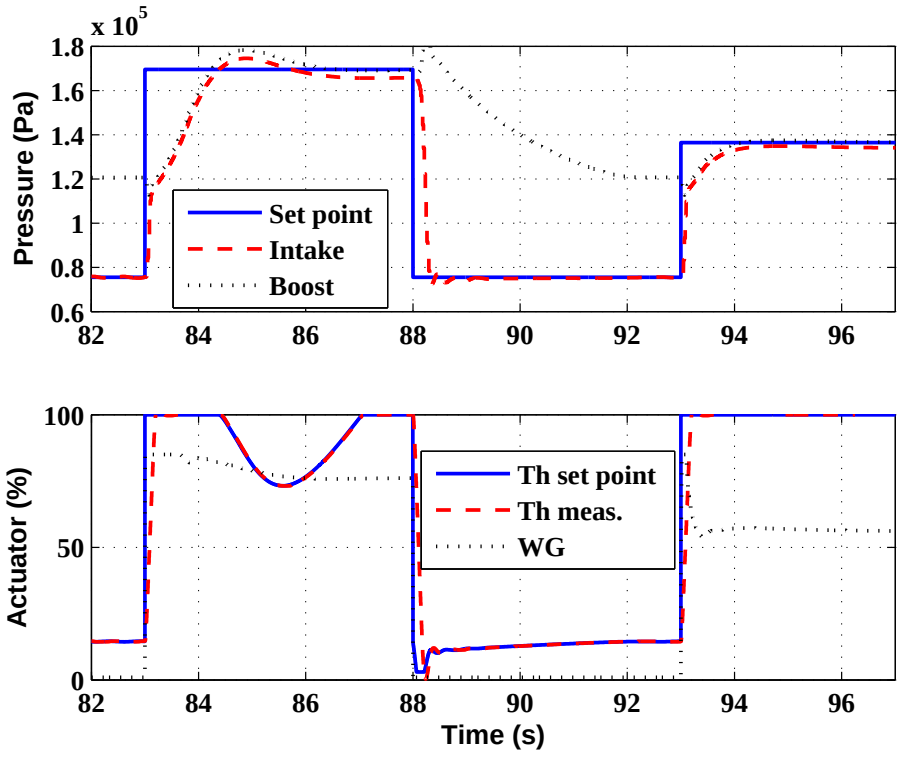

Figure 16: Simulation results at 2500rpm. Pressure (Pa) vs. time (s) (top): set point p_{man_sp} (blue solid), intake manifold p_{man} (red dash), boost p_{boost} (red dash); Actuator position (%) vs. time (s) (bottom): throttle set point (blue solid), throttle position (red dash), wastegate closing (black dot)

- variation of intake manifold pressure set point at a fixed engine speed (2500 rpm) (Figures 20 and 21)

Figure 17 shows the intake manifold pressure set point p_{man_sp} and the intake manifold pressure p_{man} when the torque target changes. Figure 18 shows the actuators response and figure 19 shows the engine speed during the same test. As the performances are quite correct in terms of intake manifold pressure, torque is well controlled. Nevertheless, some pressure oscillations appears due to throttle oscillations around limp-home position (around 360s) and an overshoot of 70mbar can seen at 360s that could be suppressed while filtering the set point (as used in industry). In this test, the turbocharger controller fixes naturally the wastegate fully opened which correspond to 0%.

Figure 20 shows the intake manifold pressure set point p_{man_sp}, the boost pressure p_{boost} (which cannot be less than $p_{amb} \approx 1$bar) and the intake manifold pressure p_{man} when the torque target changes. Figure 21 shows the actuators response during the same test and the contributions of the feed-forward, which is not negligible. Some boost pressure oscillations appears at 25s because of pumping turbocharger problem (no dump valve on this engine) which have a consequence on intake manifold pressure. As in simulation, small overshoots of boost pressure appear (at 17s and 21s) and there is no steady state error (e.g. at 24s) except between 26s and 30s where boost pressure cannot reach the target because wastegate is already fully opened. Note that the throttle is opened as wide as possible at steady state (at 24s on figure 21), because $p_{man} \approx p_{boost}$ so that the objectives are satisfied. A comparison between the proposed control and the control scheme presented in [9] is shown on figure 20 for intake manifold pressure. On can see that

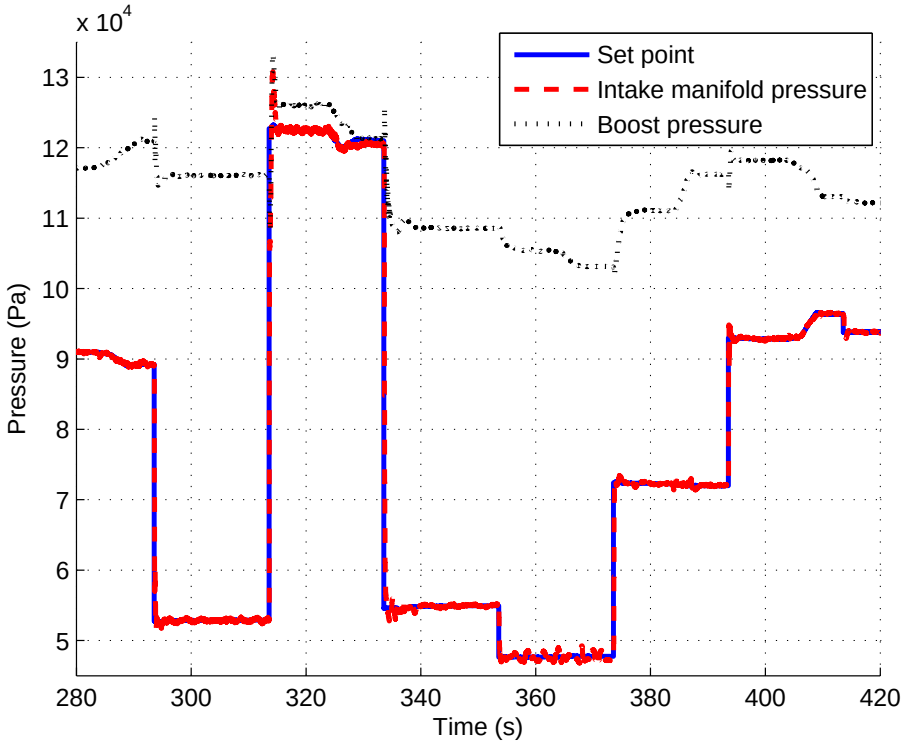

Figure 17: Pressure (Pa) results vs. time (s) on the engine test bench: set point (blue solid), intake manifold pressure (red dash), boost pressure (black dot)

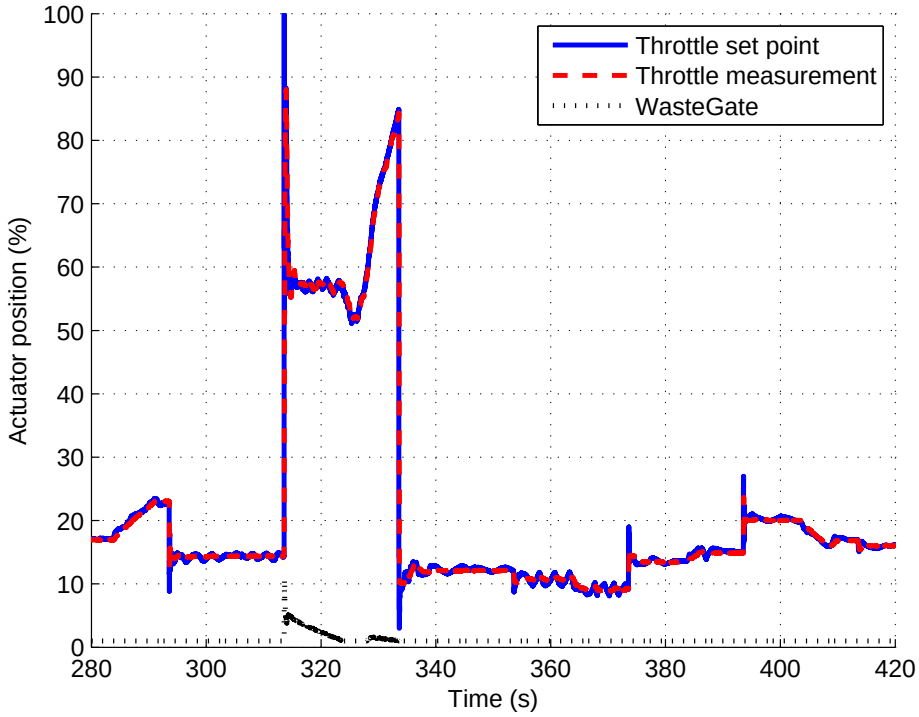

Figure 18: Actuator (%) results vs. time (s) on the engine test bench: throttle set point (blue solid), throttle position (red dash), wastegate closing (black dot)

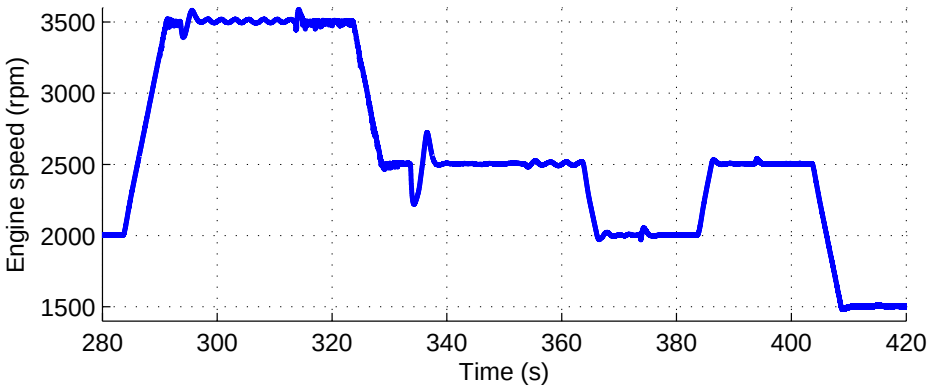

Figure 19: Engine speed (rpm) vs. time (s) on the engine test bench

the results with the proposed control scheme gives more longer overshoots (e.g. at 12s) that the results obtained with [9]. Nevertheless, this overshoot of 35mbar can be considered as acceptable.

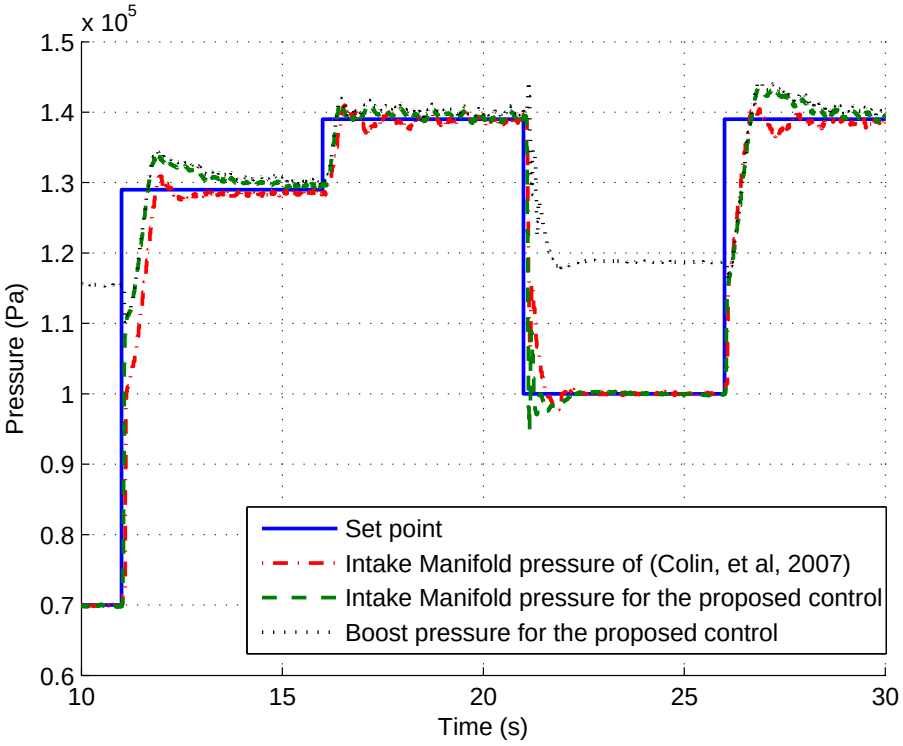

Figure 20: Pressure (Pa) results vs. time (s) on the engine test bench: set point (blue solid), p_{man} with control proposed in [9] (red dash dot), p_{man} with proposed control (green dash), p_{boost} with with proposed control (black dot)

7. Conclusion

In this paper, we have proposed a simple method for designing a robust controller that can be used on nonlinear systems. This computationally inexpensive controller is thus obtained faster and more systematically than the

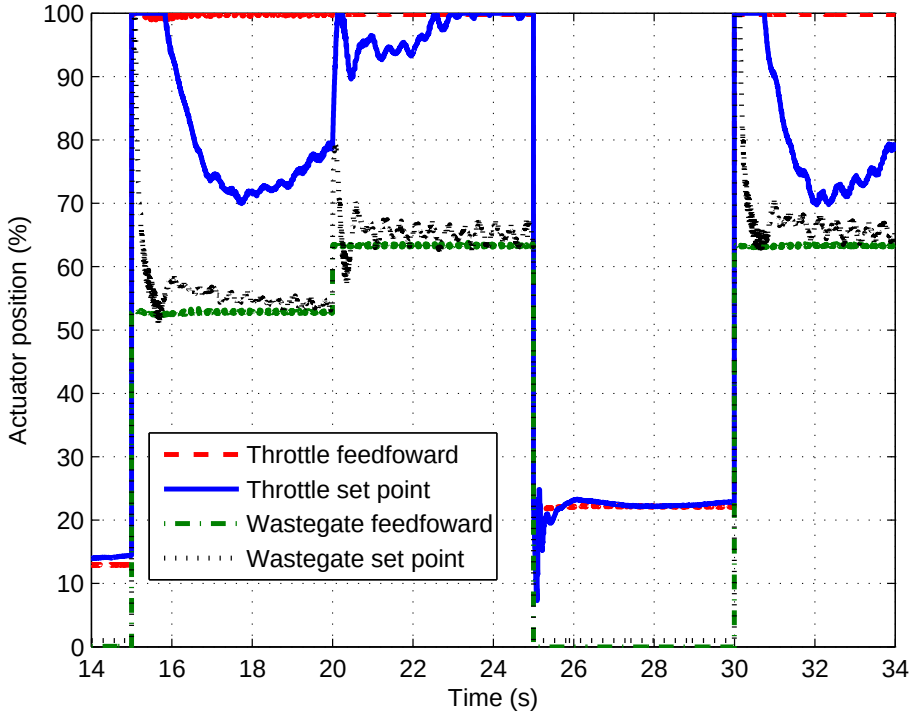

Figure 21: Actuator (%) results vs. time (s) on the engine test bench: throttle feedforward (red dash), throttle set point (blue solid), wastegate feedfoward (green dash dot), wastegate closing (black dot)

usual look-up-table based controllers. The successive steps of the method are: system identification, system normalization and linearization, nominal model design, model uncertainty design, and controller design with property verification. The system has been normalized and linearized so that any linear controller, available in the linear control theory literature, could be used in the control scheme. The classical PID controller, tuned with a pole placement method in which robustness is verified, is chosen here for its simplicity and in order to prove the effectiveness of the proposed method. This robust control methodology has been applied to the air path of a downsized spark ignition engine, i.e. intake manifold pressure control and boost pressure control. The good control performances of the proposed method have been demonstrated first in simulation and next on an engine test bench.

References

[1] B. Lecointe, G. Monnier, Downsizing a gasoline engine using turbocharging with direct injection, SAE Technical Papers, no. 2003-01-0542.

[2] P. Leduc, B. Dubar, A. Rainini, G. Monnier, Downsizing of gasoline engine - an efficient way to reduce co_2 emissions, Oil & Gas Science and Technology 58 (1) (2003) 115–127.

[3] L. Guzzella, U. Wenger, R. Martin, Ic-engine downsizing and pressure-wave supercharging for fuel economy, SAE Technical Papers, no. 2000-01-1019.

[4] L. Guzzella, C. Onder, Introduction to Modeling and Control of Internal Combustion Engine Systems, Springer, 2004.

[5] G. Colin, Y. Chamaillard, B. Bellicaud, Compromis consommation et performance pour le contrle d'un moteur turbocompress, in: Confrence Internationale Francophone en Automatique (CIFA'08), Bucharest, Romania, 2008.

[6] A. Karnik, J. Buckland, J. Freudenberg, Electronic throttle and wastegate control for turbocharged gasoline engine, in: American Control Conference, Portland, OR, USA, 2005, pp. 4434–4439.

[7] L. Eriksson, S. Frei, C. Onder, L. Guzzella, Control and optimization of turbocharged spark ignited engines, in: IFAC 15th Triennial World Congress, Barcelona, Spain, 2002.

[8] L. Lezhnev, I. Kolmanovsky, J. Buckland, Boosted gasoline direct injection engines: Comparison of throttle and vgt controllers for homogeneous charge operation, SAE Technical Papers, no. 2002-01-0709.

[9] G. Colin, Y. Chamaillard, G. Bloch, G. Corde, Neural control of fast nonlinear systems - application to a turbocharged si engine with VCT, IEEE Trans. on Neural Networks 18 (4) (2007) 1101–1114.

[10] P. Moulin, J. Chauvin, B. Youssef, Modelling and control of the air system of a turbocharged gasoline engine, in: Proceeding of the 17th World Congress IFAC, Seoul, Korea, 2008, pp. 8437–8494.

[11] R. Wakeman, D. Wright, Closed loop turbocharger control with wastegate functions, SAE Technical Paper, no. 860487 (1986) 131–135.

[12] G. Colin, Y. Chamaillard, G. Bloch, G. Corde, A. Charlet, Linearized neural predictive control. A turbocharged SI engine application, SAE

2005 Transactions Journal of Engines (2005) 101–108, SAE Technical Paper 2005–01–0046.

[13] L. Guzzella, Analysis and Synthesis of Single-Input Single-Output Control Systems, Vorlesungsskript, Zurich, 2007.

[14] L. Ljung, System Identification Theory for the User, Prentice Hall, 1999.

[15] K. J. Astrom, L. Rundqwist, Integrator windup and how to avoid it, in: Proceeding of the 1989 American Control conference, 1989, pp. 1693–1698.

List of Figures

List of Tables